Cosmic ray acceleration in the laboratory

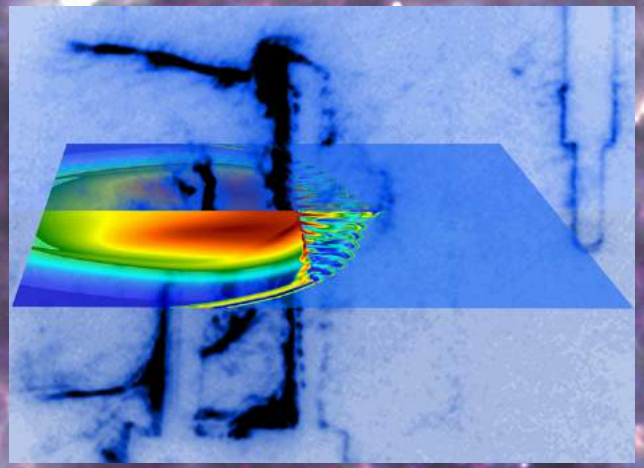

Subir Sarkar

Rudolf Peierls Centre for Theoretical Physics, Oxford
Niels Bohr Institute, Copenhagen

21st International School of Cosmic Ray Astrophysics, Erice, 1-7 August 2018

A NUMERICAL MODEL OF THE STRUCTURE AND EVOLUTION OF YOUNG SUPERNOVA REMNANTS

Mon. Not. R. astr. Soc. (1973) **161**, 47

S. F. Gull

Mon. Not. R. astr. Soc. (1975) **171**, 263

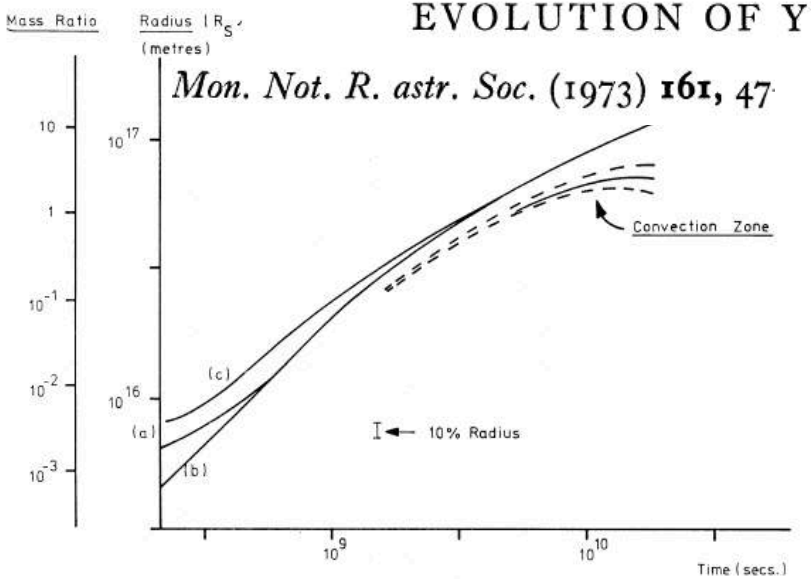

FIG. 8. *Dependence of dynamics on piston model. (i) Adiabatic lapse rate piston, $R_0 = 5 \times 10^{15}$ m. (ii) Adiabatic lapse rate piston, $R_0 = 5 \times 10^{14}$ m. (iii) Isothermal piston, $R_0 = 5 \times 10^{15}$ m.*

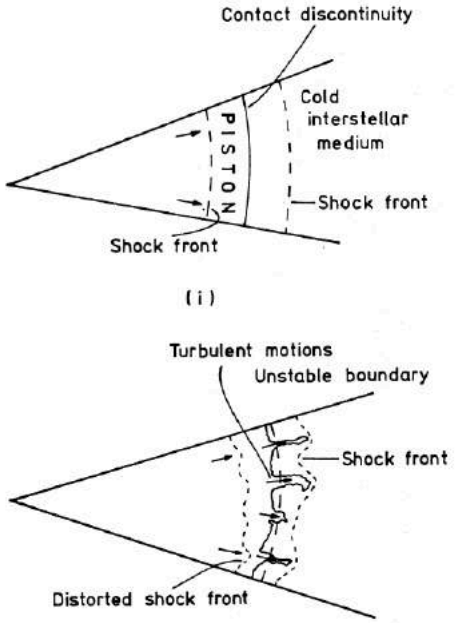

FIG. 3. (1) *Schematic structure of a young supernova remnant, showing the internal shock front.* (2) *Modification of internal structure when the contact discontinuity is distorted by the Rayleigh–Taylor instability. Some fraction of the energy now appears as random motions in the neighbourhood of the filaments.*

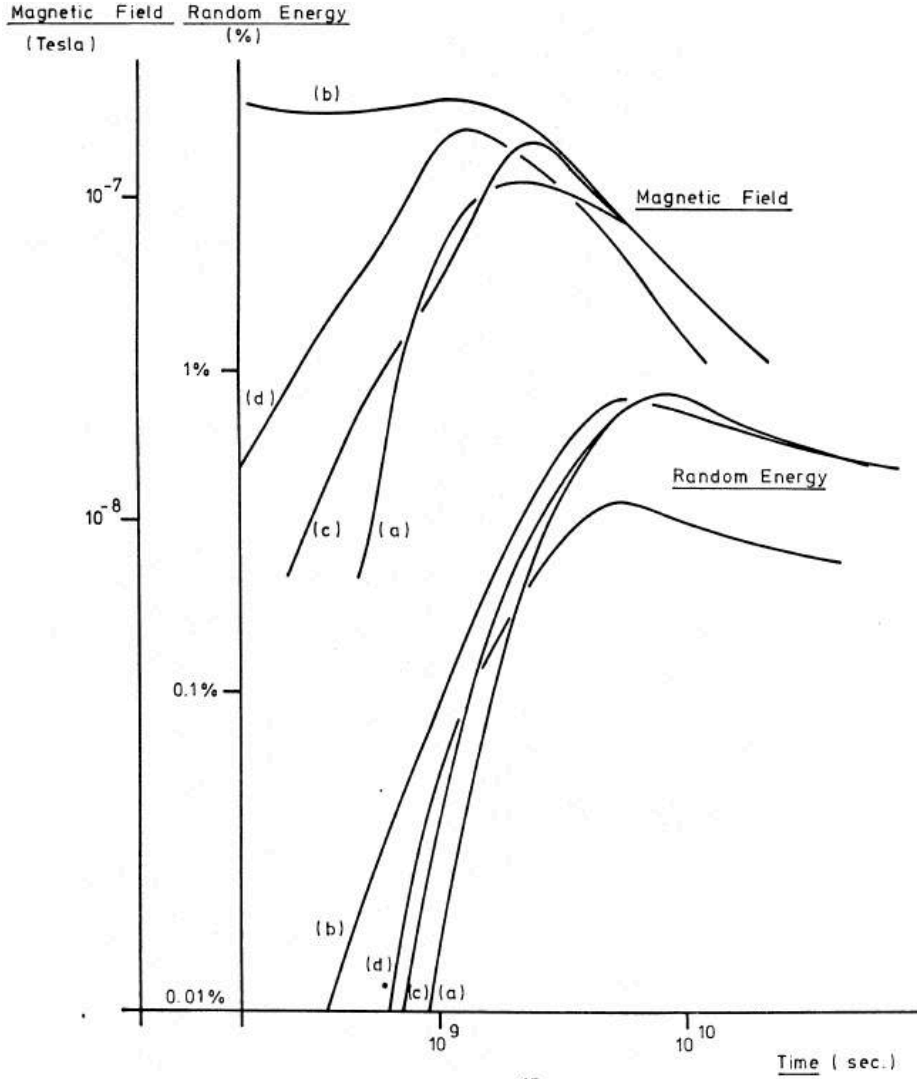

(a) Adiabatic Lapse Rate Piston, $R_0 = 5 \times 10^{15}$ m.
(b) Adiabatic Lapse Rate Piston, $R_0 = 5 \times 10^{14}$ m.
(c) Constant Density Piston
(d) Isothermal Piston

FIG. 9. *Turbulent energy and magnetic field in the convection zone. Note that, whilst the individual piston models show great differences in the early part of the evolution (particularly for small R_0) the predicted turbulent energies and magnetic fields agree to within a factor of 2 when the mass ratio is greater than 0·1 ($t > 10^9$ s).*

Turbulent amplification of magnetic fields by SNR shocks

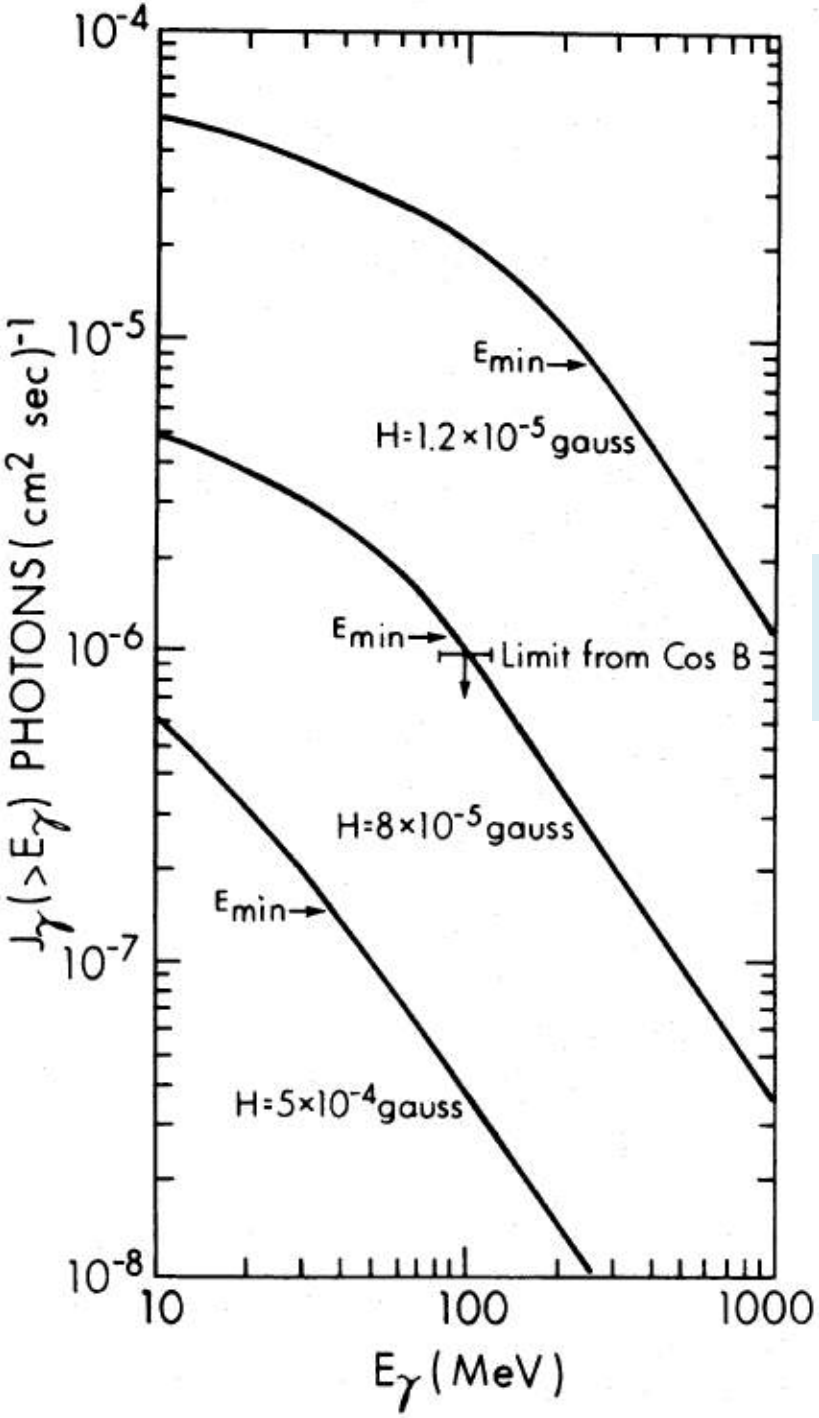

Upper limits on the γ-ray flux from Cas A (from non-thermal bremsstrahlung) did imply *amplification* of the magnetic field in the radio shell, above the compressed interstellar field … just as predicted by Gull (1973)

(Cowsik & Sarkar, MNRAS **191**:855,1980)

Relativistic electrons ✶ magnetic field → radio

" ✶ X-ray emitting plasma → γ-rays

The observational limits were subsequently tightened and MAGIC and Fermi-LAT finally *detected* γ-rays, implying a magnetic field of *O*(mG) …

Also confirmed by the thinness of the X-ray synchrotron emitting filaments

2nd-order Fermi acceleration

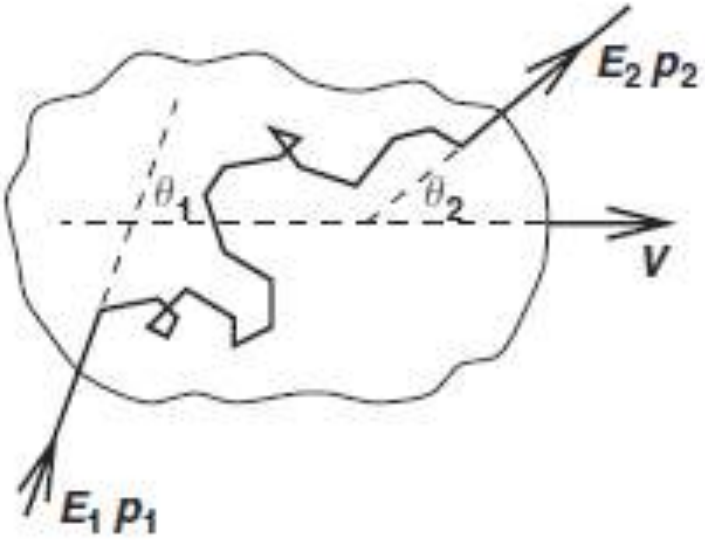

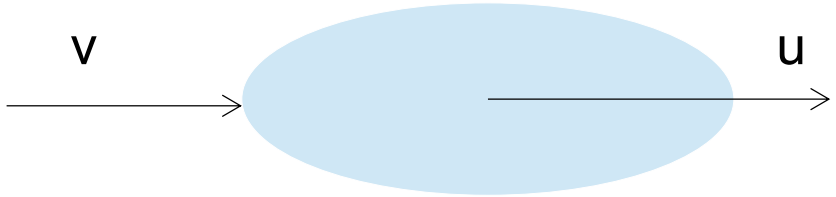

$$\delta E \sim E\left(\frac{u}{v}\right)^2$$

Fast particles collide with moving magnetised clouds (Fermi, 1949) … particles can gain *or* lose energy, but head-on collisions (⇒ gain) are more probable

It was subsequently realised that MHD turbulence or plasma waves can also act as scattering centres (Sturrock 1966, Kulsrud and Ferrari 1971)

The evolution of the particle density is governed by a diffusion equation (Kaplan, 1955)

$$\frac{\partial f}{\partial t} = -\frac{1}{p^2}\frac{\partial}{\partial p}\left(-p^2\mathcal{D}_{pp}\frac{\partial f}{\partial p}\right) - \frac{f}{\tau_{esc}} + \frac{I_0\delta(p-p_0)\delta(t-t_0)}{4\pi p^2}$$

Governing transport equation ⟹ injection + diffusion + convection + losses

$$\frac{\partial n}{\partial t} = \frac{n}{\tau_e} - \left[2K_F + \frac{1}{3}\left(\frac{d \ln B_r}{dt} - \frac{d \ln L}{dt}\right)\right] E \frac{\partial n}{\partial E} + K_F E^2 \frac{\partial^2 n}{\partial E^2} + I(\epsilon, t),$$

By making the following integral transforms …

$$n = n' \exp\left[-\int_{t_0}^{t} \frac{dt'}{\tau_e(t')}\right],$$

$$x = E \exp\left[-\int_{t_0}^{t} \left\{2K_F(t') + \frac{1}{3}\left[\frac{d \ln B_r(t')}{dt'} - \frac{d \ln L(t')}{dt'}\right]\right\} dt'\right],$$

$$y = \exp\left[\int_{t_0}^{t} K_F(t')\, dt'\right].$$

The Green's function is obtained to be: $$G' = \frac{1}{\sqrt{4\pi y}} \exp\left[-\left(\ln \frac{x}{x_0} - y\right)^2 / 4y\right].$$

So the energy spectrum is: $$n(\epsilon, t) = \int_{t_0}^{t} dt'_0 \int_{-\infty}^{\infty} d\epsilon'_0\, \tilde{G}(\epsilon, \epsilon'_0, t, t'_0)\, I(\epsilon'_0, t'_0).$$

Cowsik & Sarkar, MNRAS **207**:745,1984

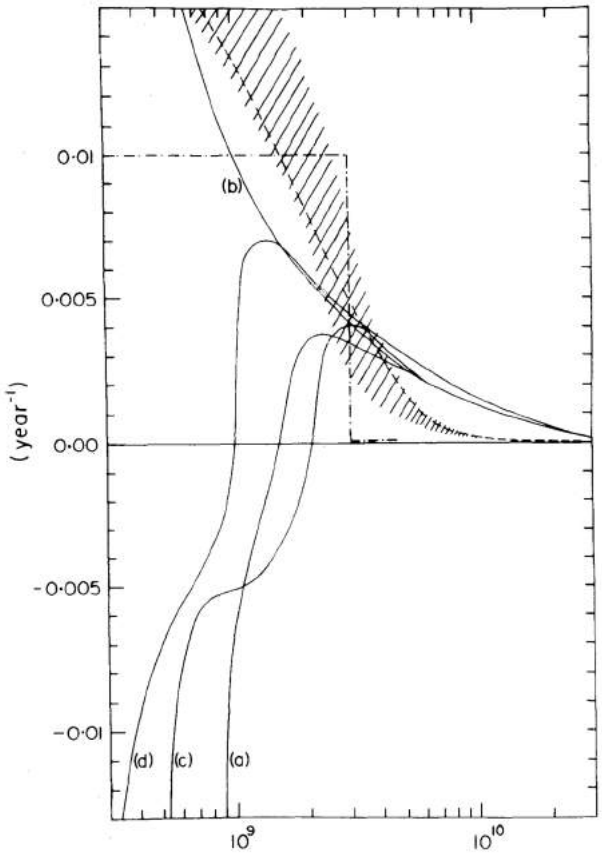

Figure 2. Time variation of the secular deceleration rate,

$$\frac{1}{3}\left(\frac{d \ln L}{dt} - \frac{d \ln B_r}{dt}\right),$$

for the 'piston models' of Fig. 1. The hatched area is the envelope of the time variation of K_F, the stochastic acceleration rate, for models (c) and (d). The dashed line represents:

$$K_F(t) = K_1 \exp(-t/t_1) + K_2(t), \qquad K_2 \ll K_1$$

(for $K_1 = 2.2 \times 10^{-2}\,\mathrm{yr}^{-1}$; $t_1 = 2 \times 10^9\,\mathrm{s}$; $K_2 = 3.5 \times 10^{-5}\,\mathrm{yr}^{-1}$).

The dot-dashed line is the step function,

$$K_F(t) = K_0, \qquad t \leqslant t'$$
$$= K_0', \qquad t > t', \qquad K_0' \ll K_0$$

(for $K_0 = 10^{-2}\,\mathrm{yr}^{-1}$; $t' = 10^9\,\mathrm{s}$; $K_0' = 10^{-4}\,\mathrm{yr}^{-1}$).

Cowsik & Sarkar, MNRAS **207**:745,1984

→ An approximate power-law spectrum at late times, with *convex* curvature

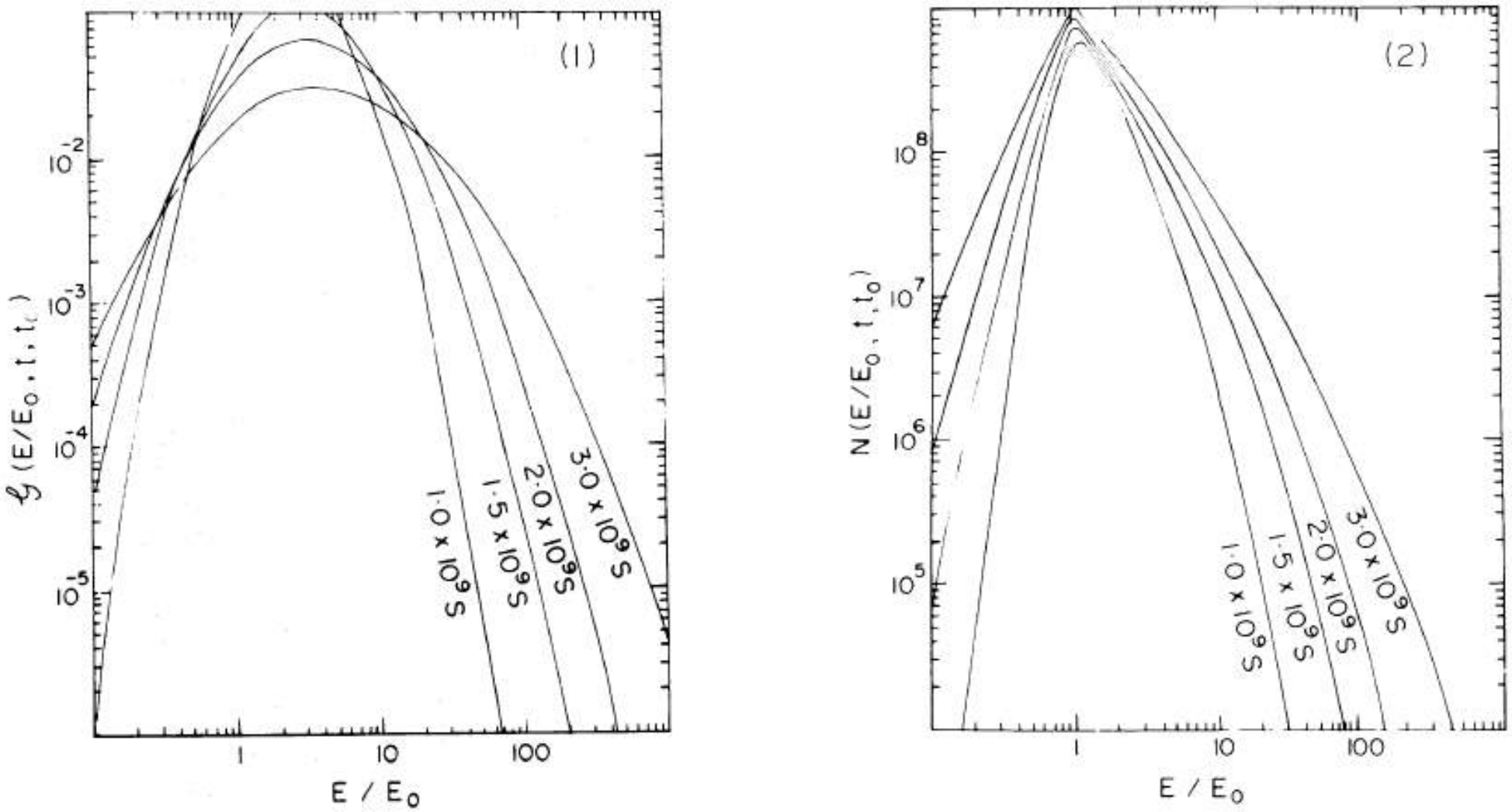

Figure 3. Evolution of the energy spectrum of particles corresponding to (1) Impulsive injection (of 1 particle) and (2) continuous injection (of 1 particle s^{-1}), for a constant rate of stochastic acceleration, $K_0 = 10^{-2}$ yr^{-1}. [Piston model (a); $t_0 = 10$ yr; $\tau_e \gg t$.]

Cowsik & Sarkar, MNRAS **207**:745,1984

The synchotron radiation spectrum depends on the electron acceleration time-scale … and *hardens* with time

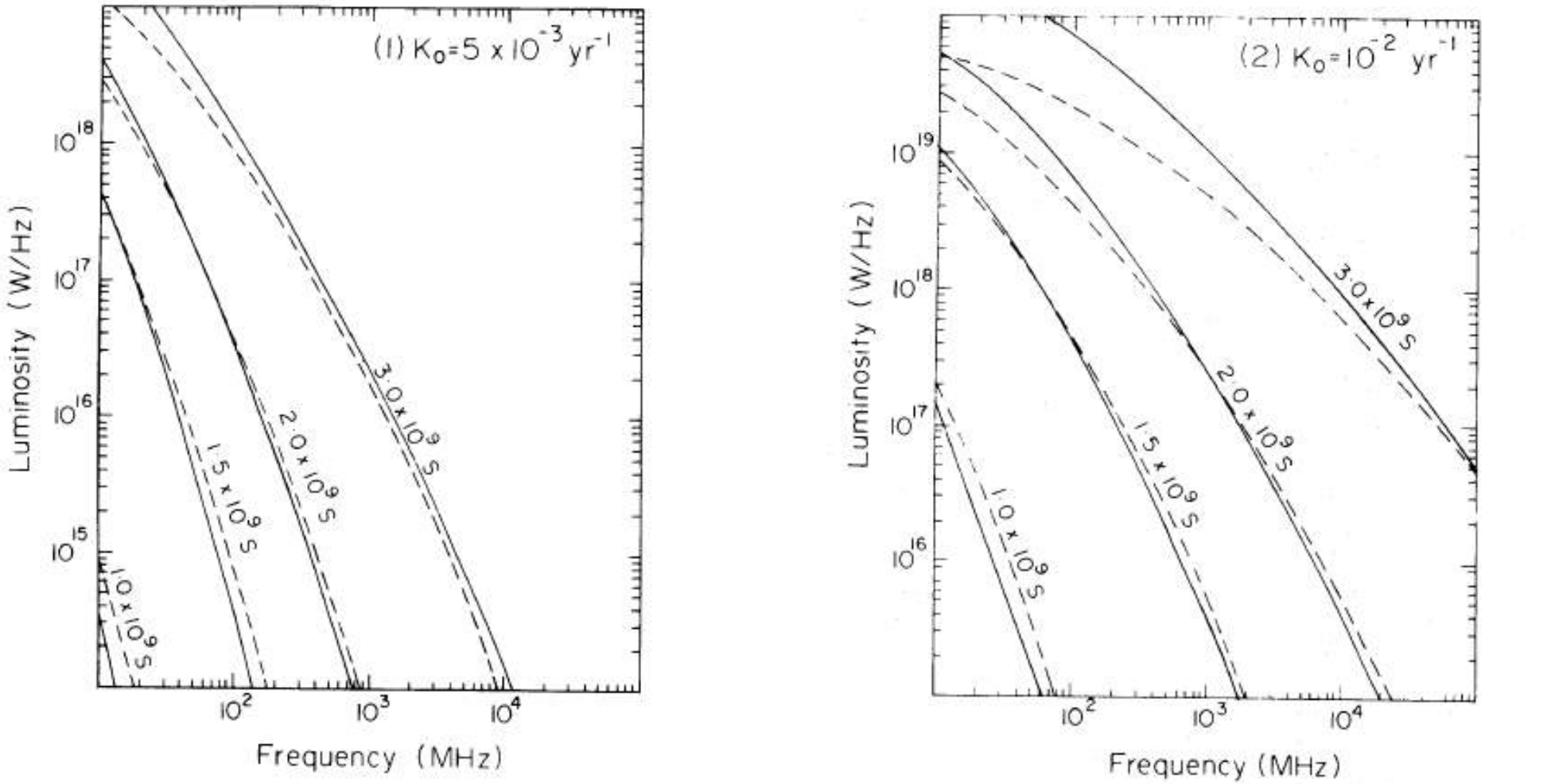

Figure 4. Evolution of the synchrotron spectrum corresponding to impulsive injection (dashed line, $E_{inj} = 10^{46}$ erg) and continuous injection at a constant rate (solid line, $\dot{E}_{inj} = 10^{38}$ erg s^{-1}), for various values of the (constant) stochastic acceleration rate, K_0. [Piston model (a): $t_0 = 10$ yr; $E_0 = 1$ MeV, $\tau_e \gg t$.]

Cowsik & Sarkar, MNRAS **207**:745,1984

The synchrotron radio spectrum of Cassiopea A is a *convex* power-law

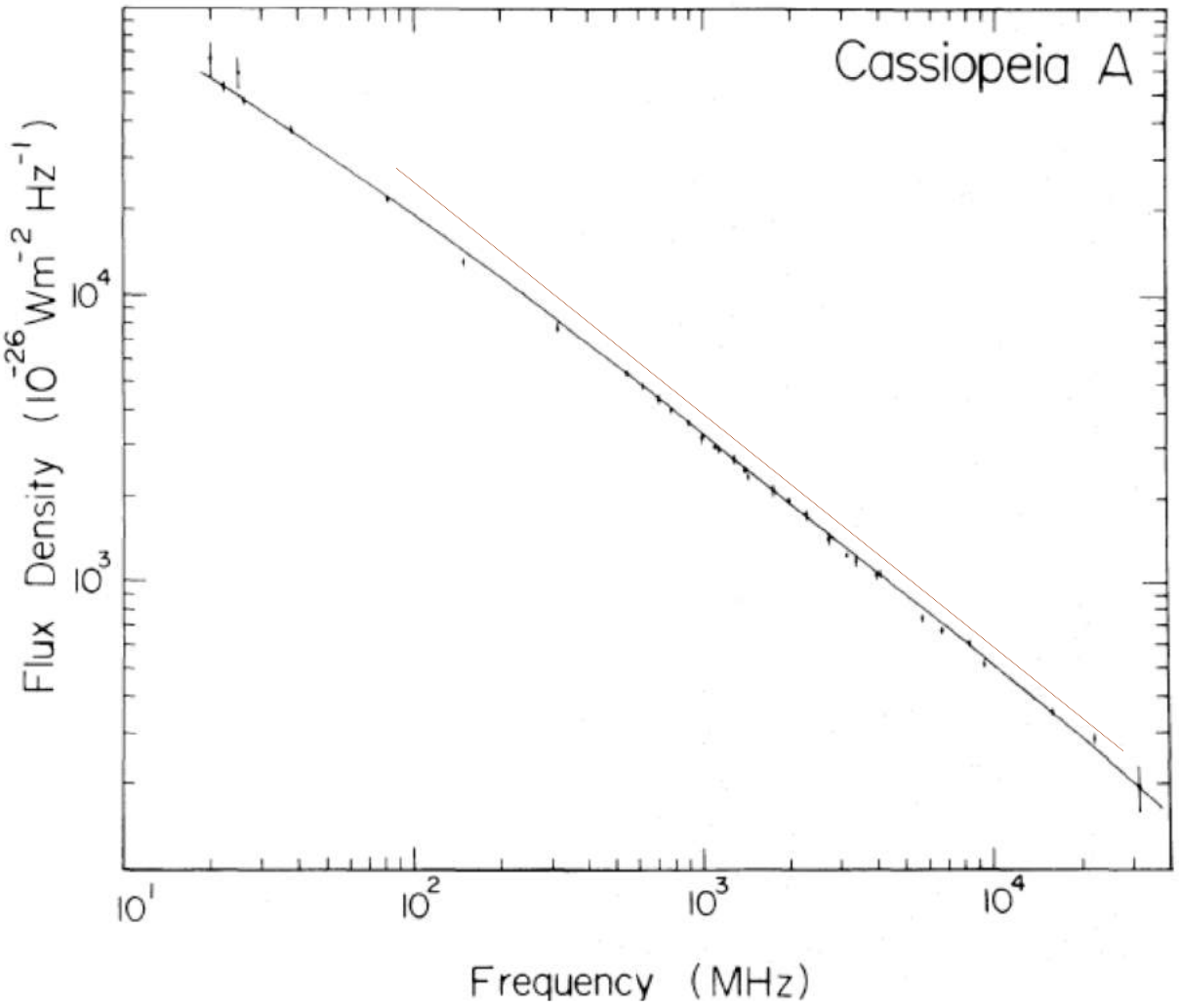

Cowsik & Sarkar, MNRAS **207**:745,1984

… perfectly fitted by the log-normal spectrum expected from *2nd order* Fermi acceleration by MHD turbulence due to plasma instabilities *behind* the shock

(NB: efficient 1st-order shock acceleration should give a *concave* spectrum!)

This also fits the observed flattening of the spectrum with time

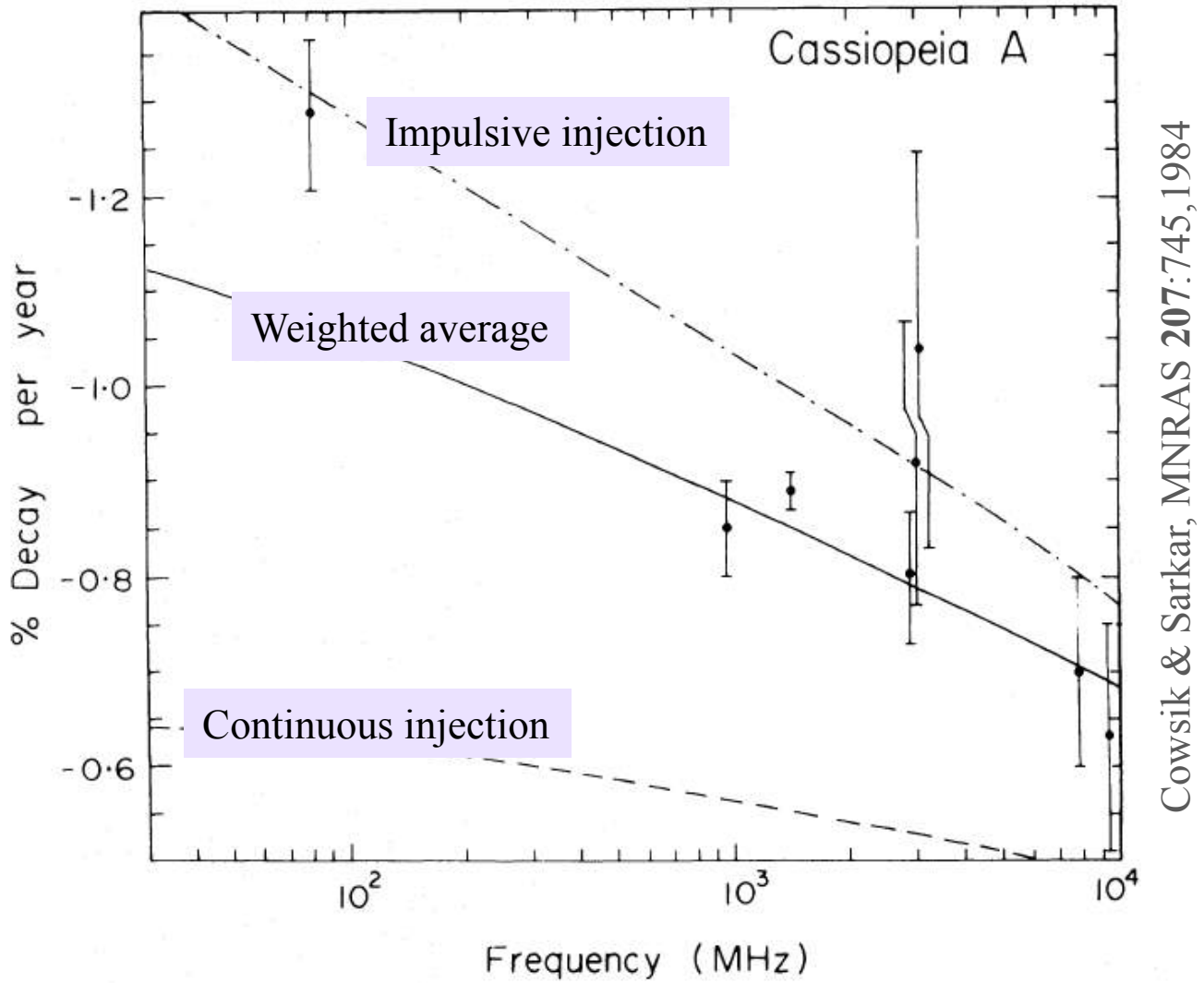

Cowsik & Sarkar, MNRAS **207**:745,1984

Figure 7. The expected decay rate of the Cas A spectrum as a function of frequency is shown separately for the cases with (dashed line) and without (dot-dashed line) continuing injection of low-energy electrons, assuming identical expansion rates. The solid line is the weighted average of the two curves (in the ratio 1: 2) and represents the decay rate of the total flux, assuming a third of it to arise from regions where low-energy particles are injected (see text for details). Observational data are from Baars *et al.* (1977).

To simulate 2nd-order Fermi acceleration in the laboratory we need a *powerful* laser to create a turbulent plasma

The laser bay at the National Ignition Facility, Lawrence Livermore National Laboratory consists of 192 laser beams delivering 2 MJ of laser energy in 20 ns pulses. The power delivered exceeds by several orders of magnitude that of the entire US national grid.

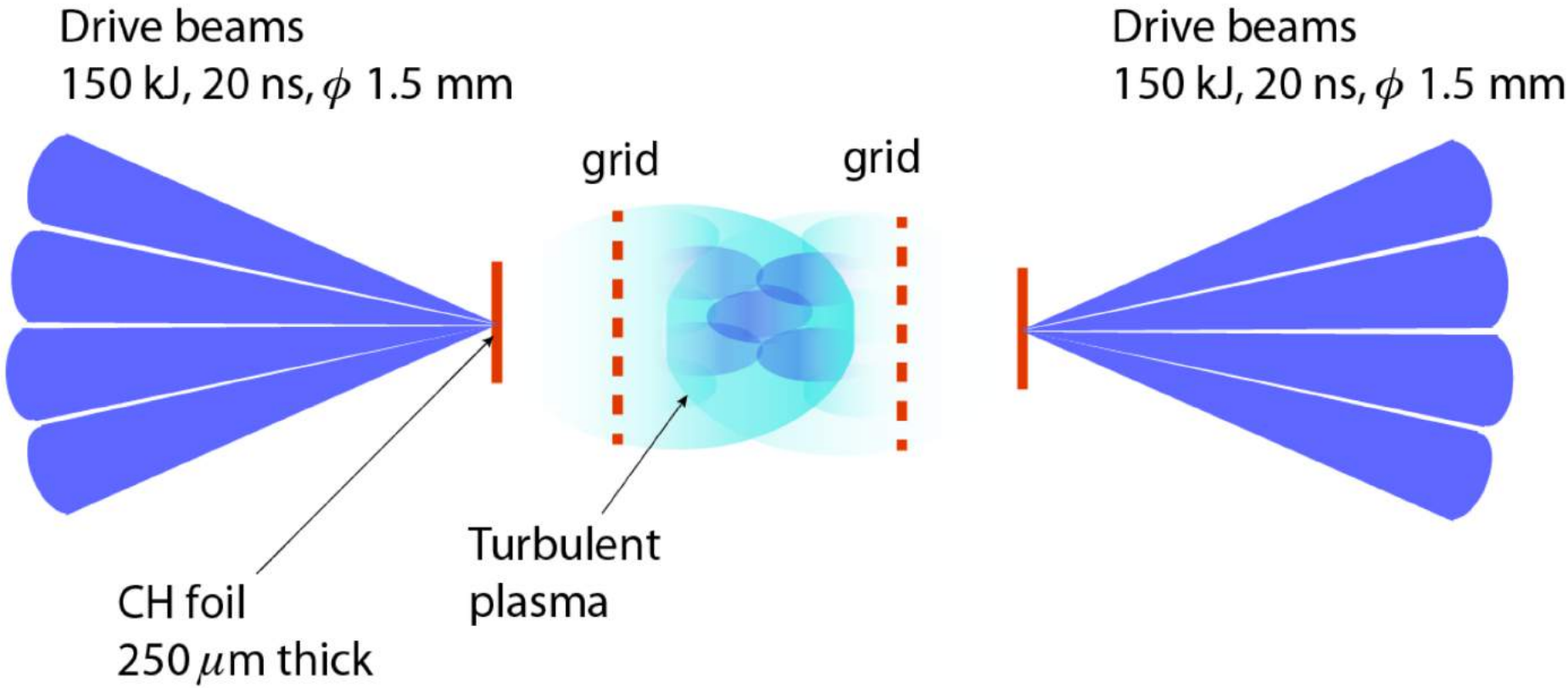

RMS magnetic field	$B \sim 1.2\,\mathrm{MG}$
mean turbulent velocity	$u = 0.002c$
scale of the turbulence cells	$\ell \sim 0.06\,\mathrm{cm}$
plasma size	$L = 0.4\,\mathrm{cm}$
initial proton momentum	$p_0 = 0.002\,m_p c$
density relation	$\nabla n/n \sim O(1)$
temperature	$T = 700\,\mathrm{eV}$

Table 1: The expected plasma parameters for the proposed experiment at the NIF, LLNL. These are derived from experiments done at other facilities Tzeferacos *et al.* (2018), rescaled to NIF laser drive conditions.

Use colliding flows & grids to create strong turbulence

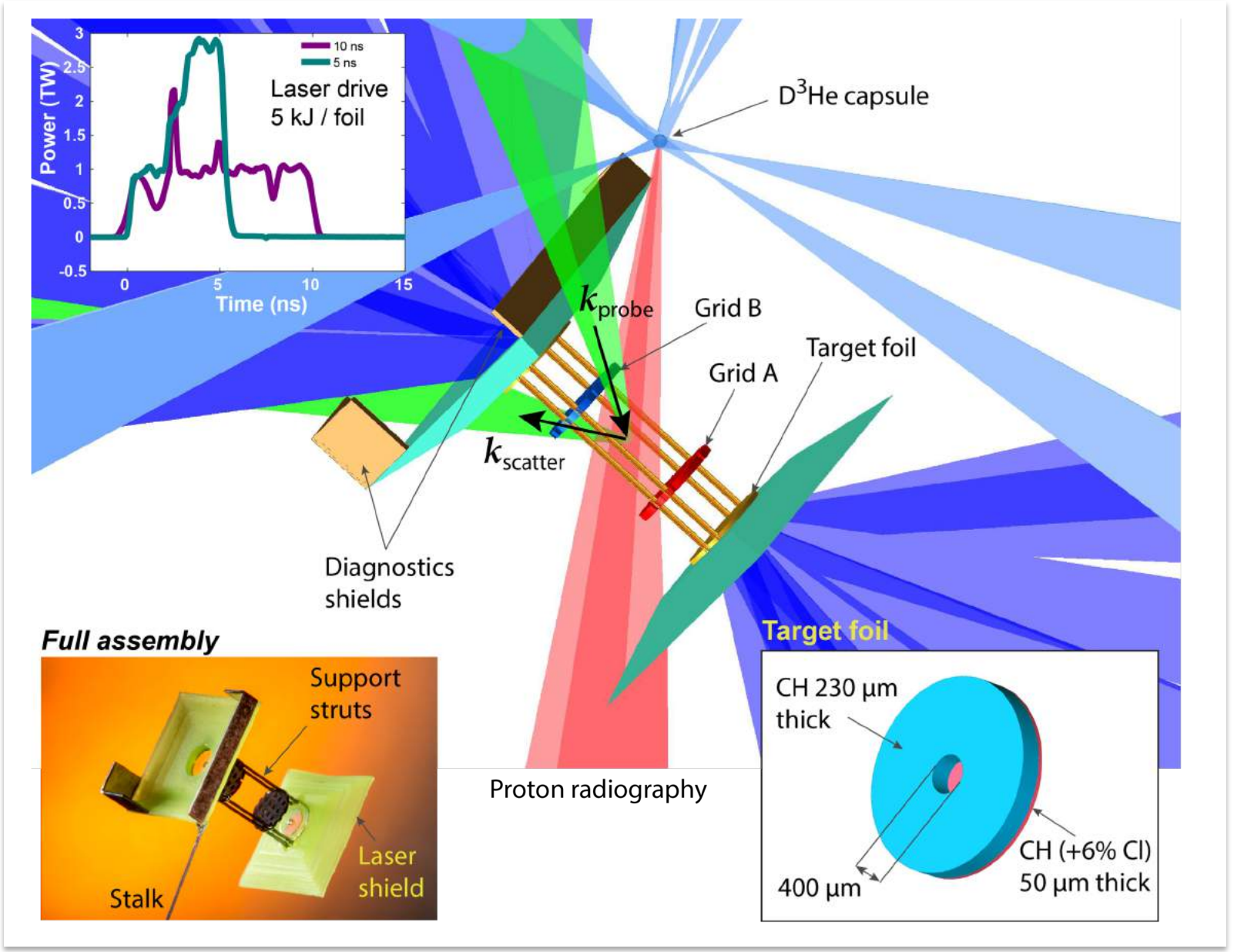

Tzeferacos *et al.* Nature Comm. (2018)

The colliding flows contain D and ~3 MeV protons are produced via D+D → T + p reactions

Fokker-Plank diffusion coefficients

- Diffusion coefficient $D_\varepsilon = \dfrac{\langle(\Delta\varepsilon)^2\rangle}{\Delta t} = \dfrac{p^2}{m_p^2} D_p$

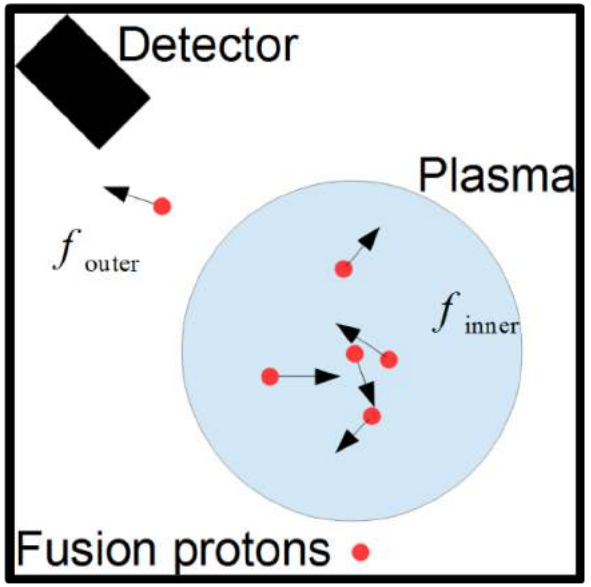

- Ohm's law

$$\mathbf{E} = -\mathbf{u}\times\mathbf{B} - \beta\frac{\delta_i}{l}\nabla P_e + \frac{\delta_i}{l}\mathbf{j}\times\mathbf{B} + \frac{1}{R_m}\mathbf{j} + \left(\frac{\delta_e}{l}\right)^2\frac{\partial\mathbf{j}}{\partial t}$$

Taking the fields and flows to be uncorrelated over one cell size, the momentum diffusion coefficient is:

$$D_p = \frac{l}{c}\left(\frac{4e^2B^2}{3}\frac{u^2}{c^2} + e^2T^2\left(\frac{\nabla n}{n}\right)^2\right)\frac{m_p c}{p}$$

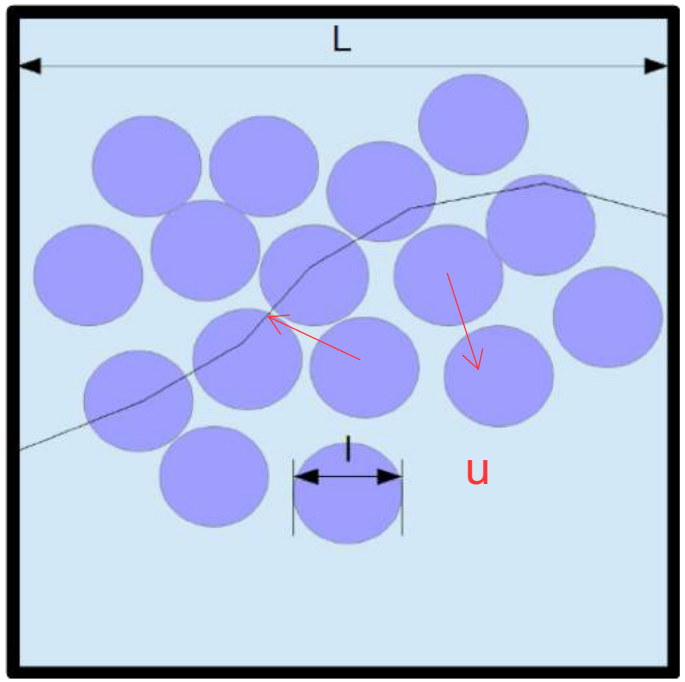

And the spatial diffusion coefficient is:

$$D_x = \frac{m_p^2 c^5}{3q^2 l B^2}\left(\frac{p}{m_p c}\right)^3 \qquad \tau_{esc} = \frac{L^2}{D_x}$$

Relevant time scales

- Streaming time $\tau_{cross} = 1.7\times10^{-10}s$
- Scattering time $\tau_{90} = 1.5\times10^{-10}s\left(\frac{B}{1.2MG}\right)^{-2}\left(\frac{l}{0.1cm}\right)^{-1}$
- Escape time $\tau_{esc} = 5.5\times10^{-10}s\left(\frac{B}{1.2MG}\right)^{2}\left(\frac{l}{0.1cm}\right)$

To have diffusion, the scattering time must be *smaller* than the escape time

However the inferred parameters are on the edge between **ballistic escape** and **diffusion** … so need higher magnetic field to ensure diffusion

Parameter	**Omega facility**	**Scaled NIF value**
RMS magnetic field	0.12 MG	1.2 – 4 MG
Temperature	450 eV	700 eV
Mean turbulence velocity	150 km/s	600 km/s
Reynolds number	370	
Magnetic Reynolds number	870	

Analytic solutions to the Fokker-Planck equation

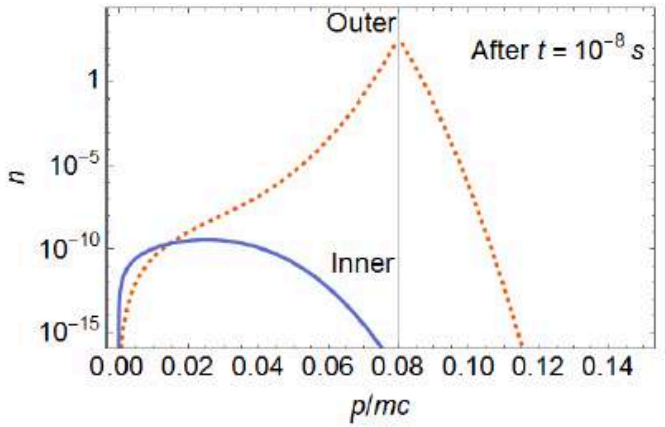

(a)

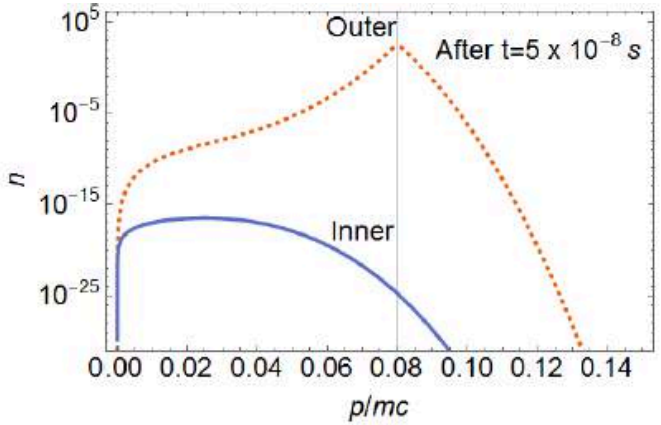

(b)

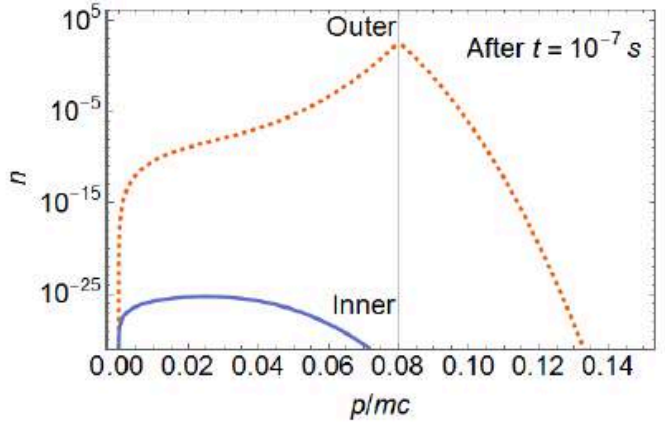

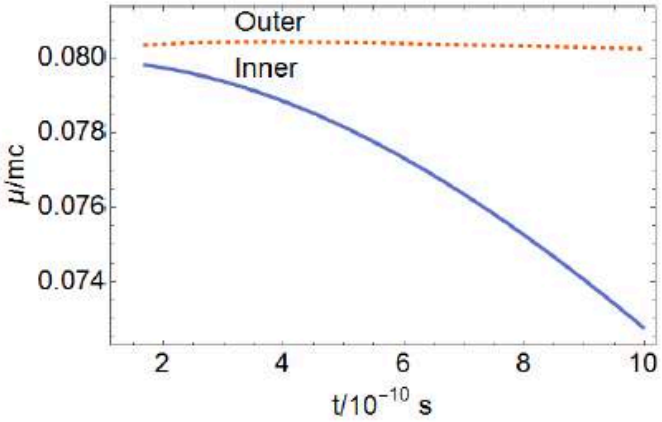

$$n_{\text{inner}} = \frac{2\hat{p}^2\sqrt{\Psi}}{\sqrt{k\tau}\,(1-\Psi)} e^{-\frac{\left(\hat{p}^3+\hat{p}_0^3\right)(1+\Psi)}{3\sqrt{k\tau}(1-\Psi)}} \mathrm{I}_0\left[\frac{4\left(\hat{p}\hat{p}_0\right)^{\frac{3}{2}}\sqrt{\Psi}}{3\sqrt{k\tau}\,(1-\Psi)}\right]$$

$$n_{\text{outer}}(p, p_0, t, t_0) = \int_0^t \frac{n_{\text{inner}}(p, p_0, t', t_0)}{\tau_{\text{esc}}}\,\mathrm{d}t'$$

Expect mean energy to increase by 10-200 keV and FWHM by 0.24-1.2 MeV – ***detectable***!

Laser experiments *can* test and validate models

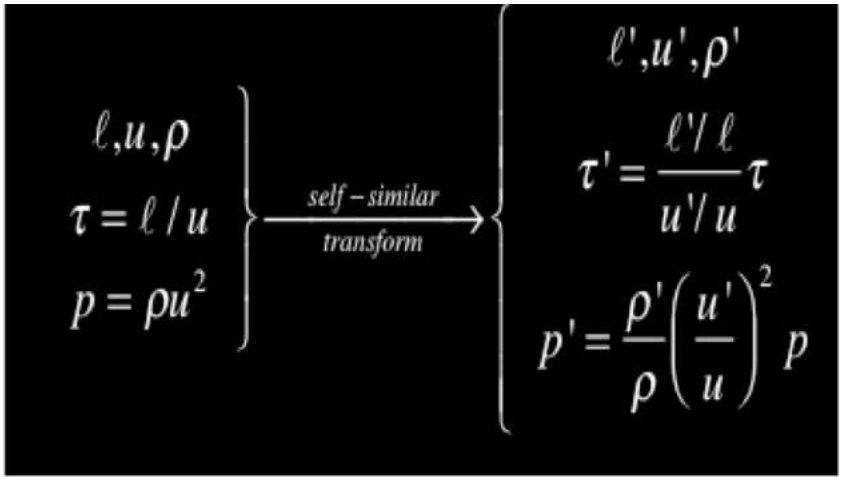

→ Equations of ideal MHD have *no* intrinsic scale, hence similarity relations exist

→ This requires that Reynolds number, magnetic Reynolds number, *etc* are all large – in both the astrophysical and analogue laboratory systems

$$\frac{\partial \rho'}{\partial t'} + \nabla' \cdot (\rho' \mathbf{u}') = 0$$

The difficulty, so far, remains in achieving these to be large enough for the dynamo to be operative

$$\rho' \left(\frac{\partial \mathbf{u}'}{\partial t'} + \mathbf{u}' \cdot \nabla' \mathbf{u}' \right) = -\nabla' P' + \frac{1}{R_e} \nabla' \cdot \boldsymbol{\sigma}' + \mathbf{F}'_{EM}$$

Reynolds number

$$\frac{\partial}{\partial t'} \left(\rho' \varepsilon' + \frac{\rho' \mathbf{u}'^2}{2} \right) + \nabla' \cdot \left(\rho' \mathbf{u}' \left(\varepsilon' + \frac{\mathbf{u}'^2}{2} \right) + P' \mathbf{u}' \right) = \frac{1}{R_e} \nabla' \cdot (\boldsymbol{\sigma}' \cdot \mathbf{u}') - \mathbf{J}' \cdot \mathbf{E}'$$

$$\frac{\partial \mathbf{B}'}{\partial t'} = \nabla' \times (\mathbf{u}' \times \mathbf{B}') + \frac{1}{R_m} \nabla'^2 \mathbf{B}'$$

Magnetic Reynolds number

Particle acceleration relies on there being a injection mechanism

- For diffusive shock acceleration to work, the particles must cross the shock *many* times i.e. their Larmor radius must exceed the shock thickness
- There must *already* be a population of energetic particles in order for the Fermi process to operate …. this is the 'injection problem'
- This pre-acceleration mechanism can be provided by wave-plasma instabilities, such as the modified two-stream instability

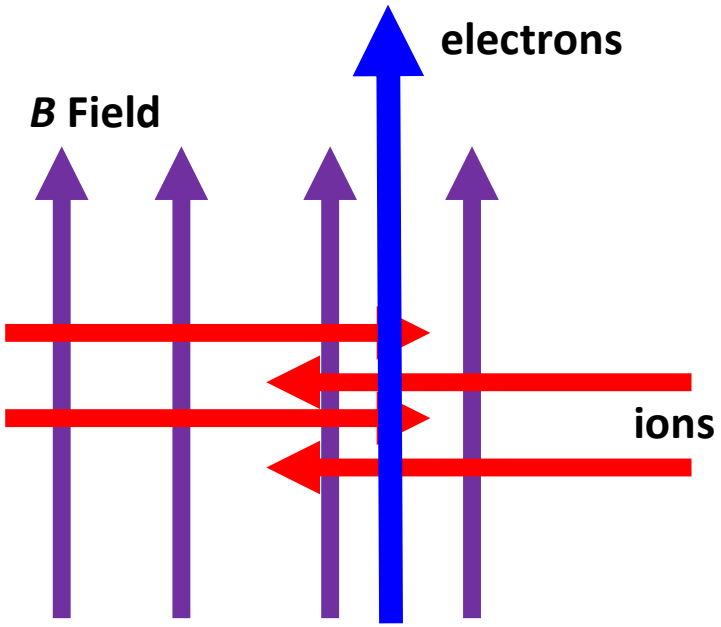

Lower-hybrid waves (at perpendicular shocks)

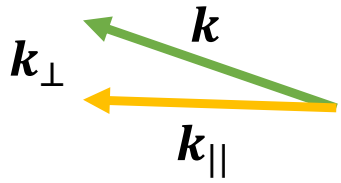

$$\omega = \boldsymbol{k}_{||} \cdot \boldsymbol{v}_i \approx \boldsymbol{k}_{\perp} \cdot \boldsymbol{v}_e$$

Waves in *simultaneous* Cherenkov resonance with ions and electrons

$$E_e \sim \alpha^{2/5} \left(\frac{m_e}{m_i}\right)^{1/5} m_i u^2$$

Laboratory experiments to investigate particle injection at shocks

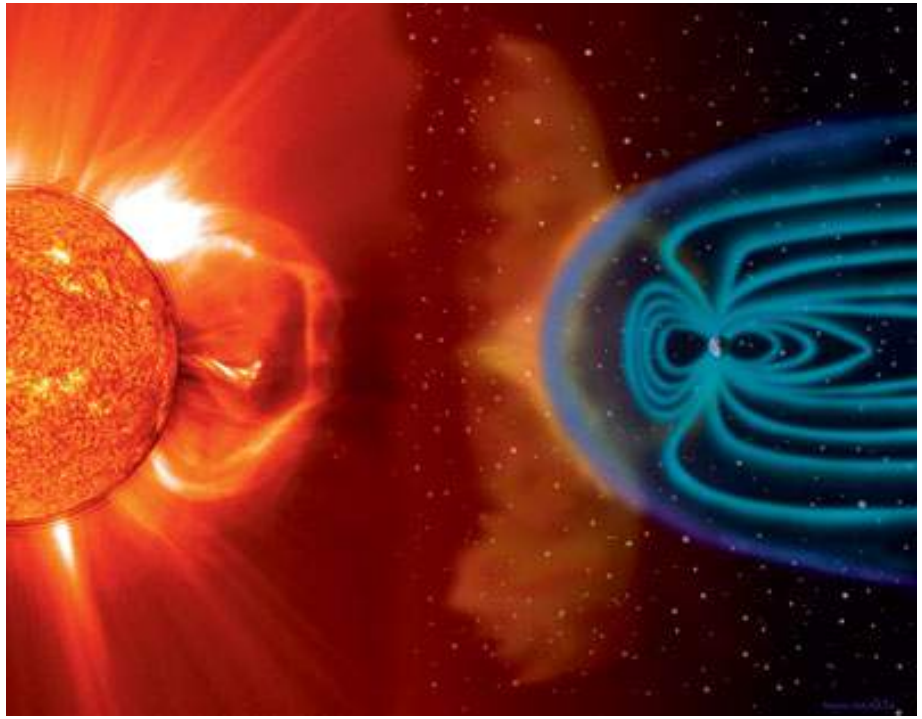

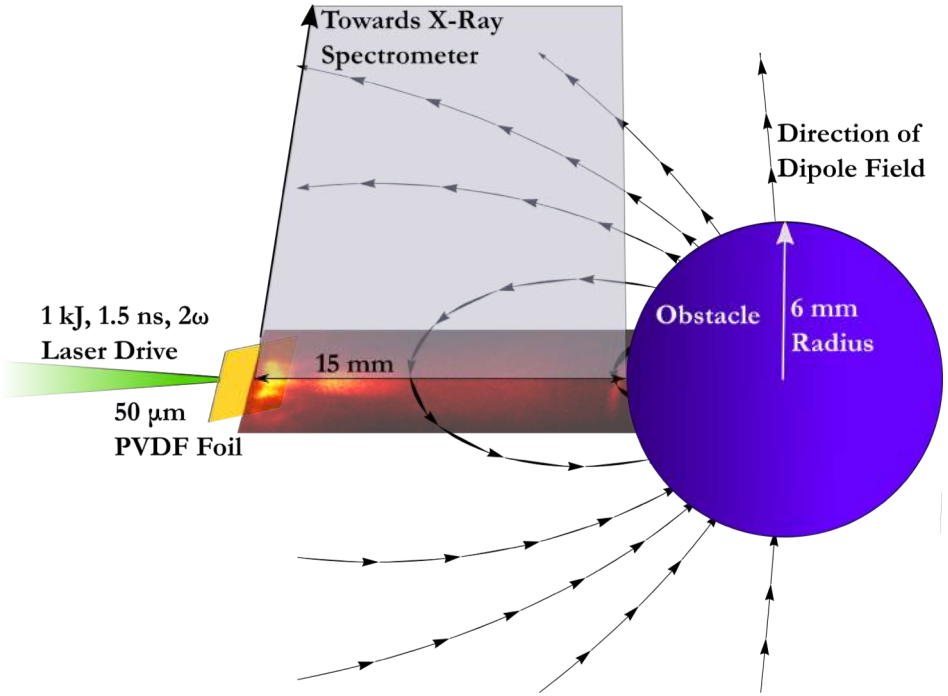

- ➜ Lower-hybrid acceleration provides a possible mechanism to pre-heat electrons above the thermal background
- ➜ This instability has been suggested to explain observed X-ray excess in cometary knots (Bingham *et al.* 2004)
- ➜ We have performed laboratory experiments to study this process

Laboratory experiments to investigate particle injection at shocks

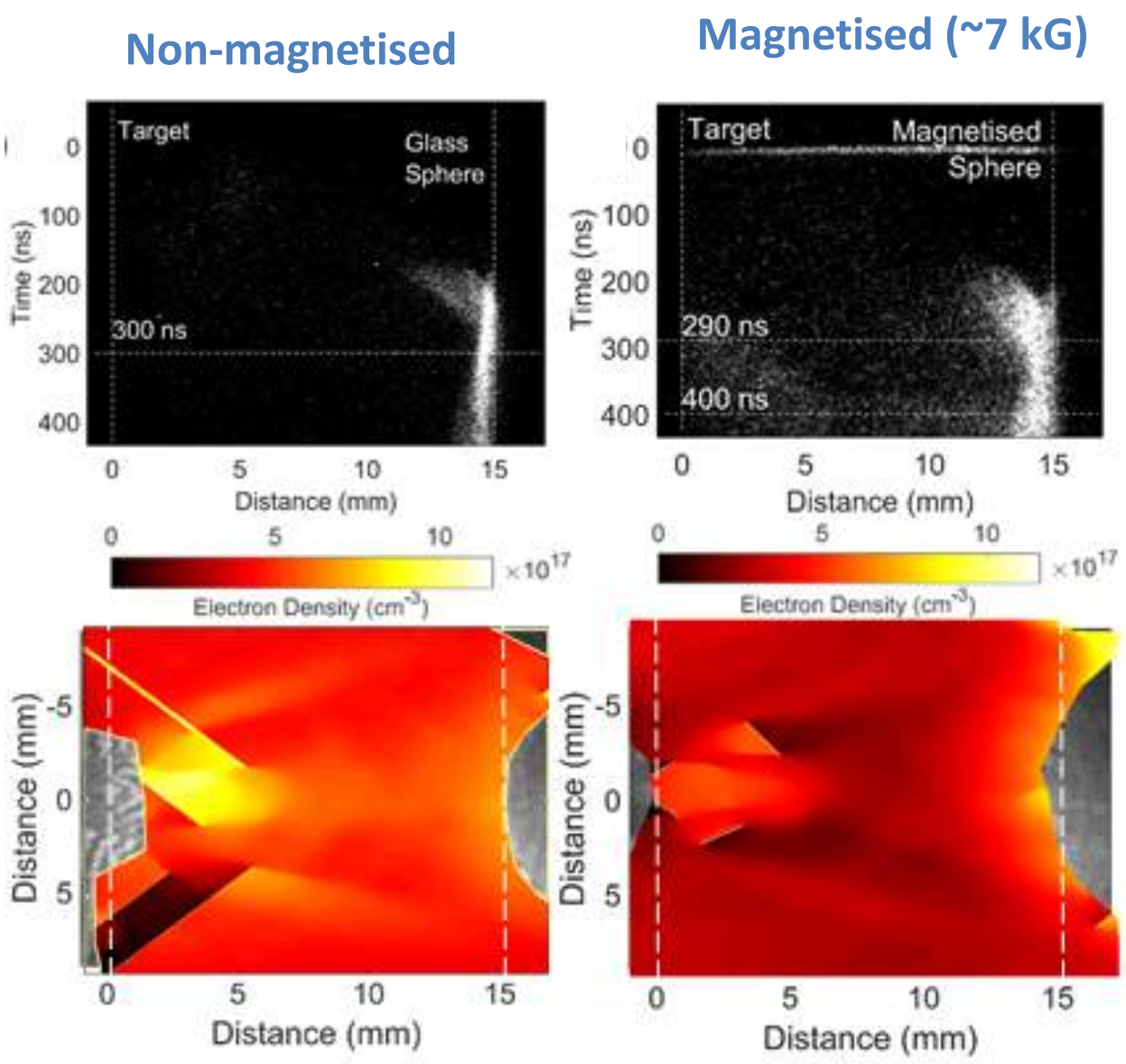

Rigby *et al*. Nature Physics (2018)

- ➜ Incoming plasma with velocity ~70 km/s
- ➜ Data shows formation of a shock when magnetic field is present
- ➜ Reflected ions have mean free path of a few mm (larger than their Larmor radius)
- ➜ Plasma $\beta \sim 0.2$ for quasi-perpendicular shock, hence magnetised two stream instability can be excited

PIC simulations show lower-hybrid heating of electrons near shock

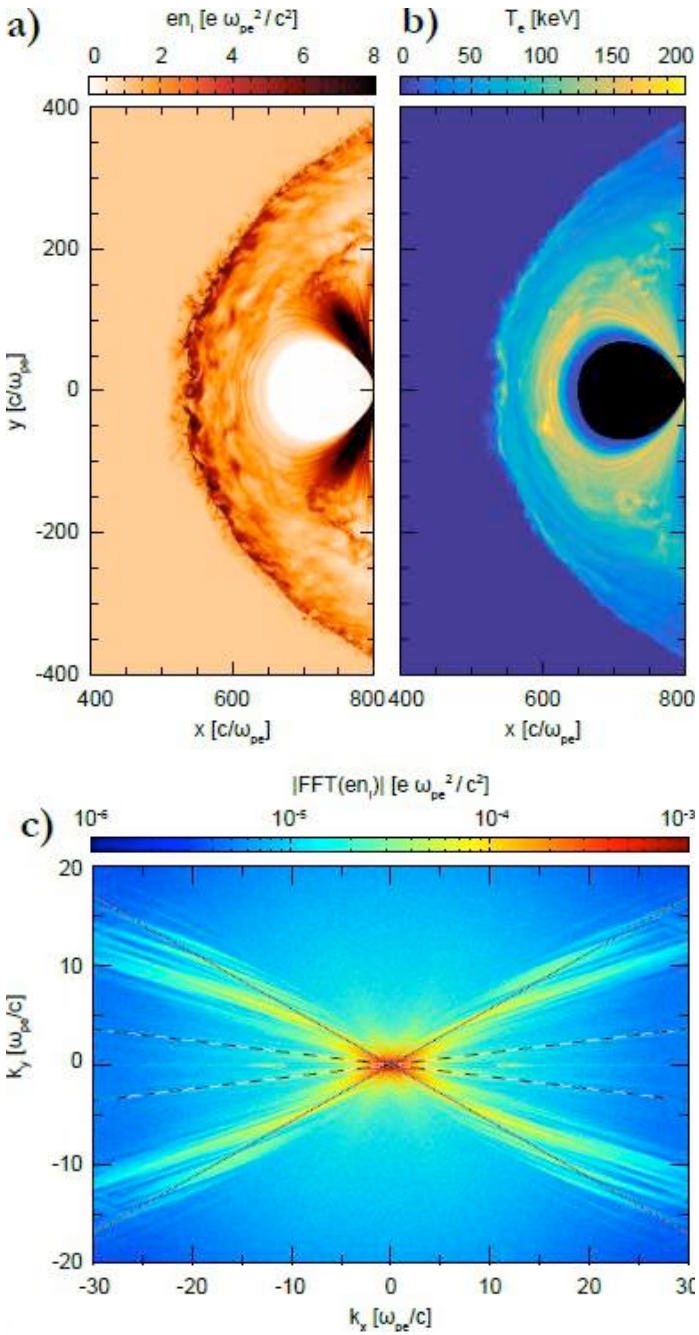

OSIRIS PIC simulations

- ➜ We have performed 2D PIC using the massively parallel code OSIRIS
- ➜ Simulations are performed with a reduced mass ratio and higher flow velocity, but Alfvenic Mach number is kept the same (scale invariance)

- ➜ Shock is formed with electron heating along B-field lines
- ➜ Turbulent wave spectrum is formed with dispersion relation consistent with LH waves

Measurement of 'cosmic ray' diffusion

- An experiment was undertaken to measure the diffusion coefficient in the plasma
- A pinhole was inserted to collimate the proton flux from an imploding D3He capsule
- Without magnetic fields, the pinhole imprints a sharp image of the pinhole onto the detector
- Random magnetic fields will induce perpendicular velocities to the protons resulting in smearing of the pinhole imprint

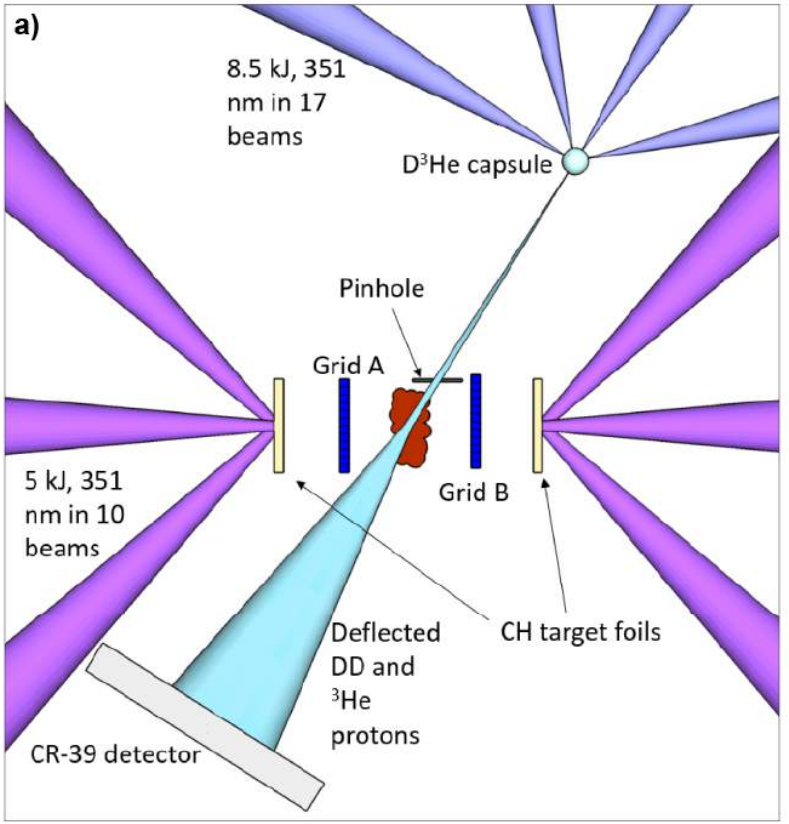

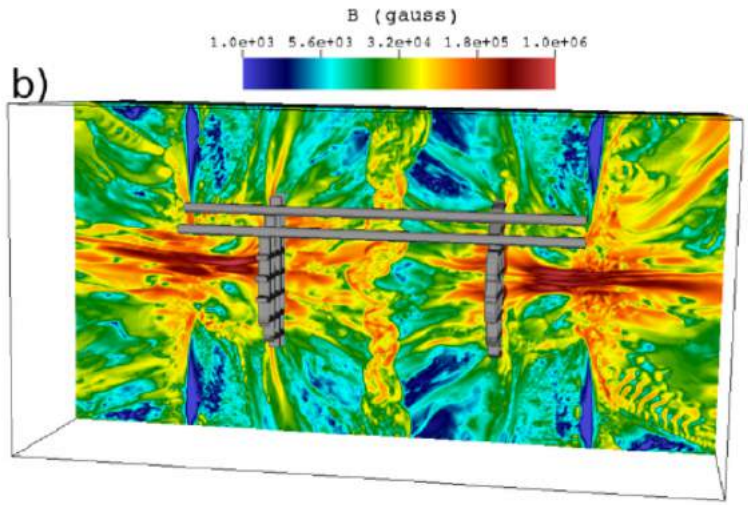

Chen *et al.,* to appear

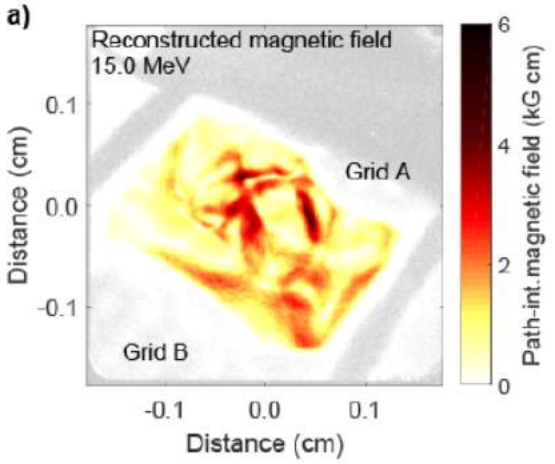

Observe *smearing* of the edges of the pinhole imprint

…. Could in principle be caused by multiple effects (turbulent fluid motions, plasma instabilities, etc) – but all can be shown to be negligible in practice

→ Can reliably ascribe to stochastic magnetic fields

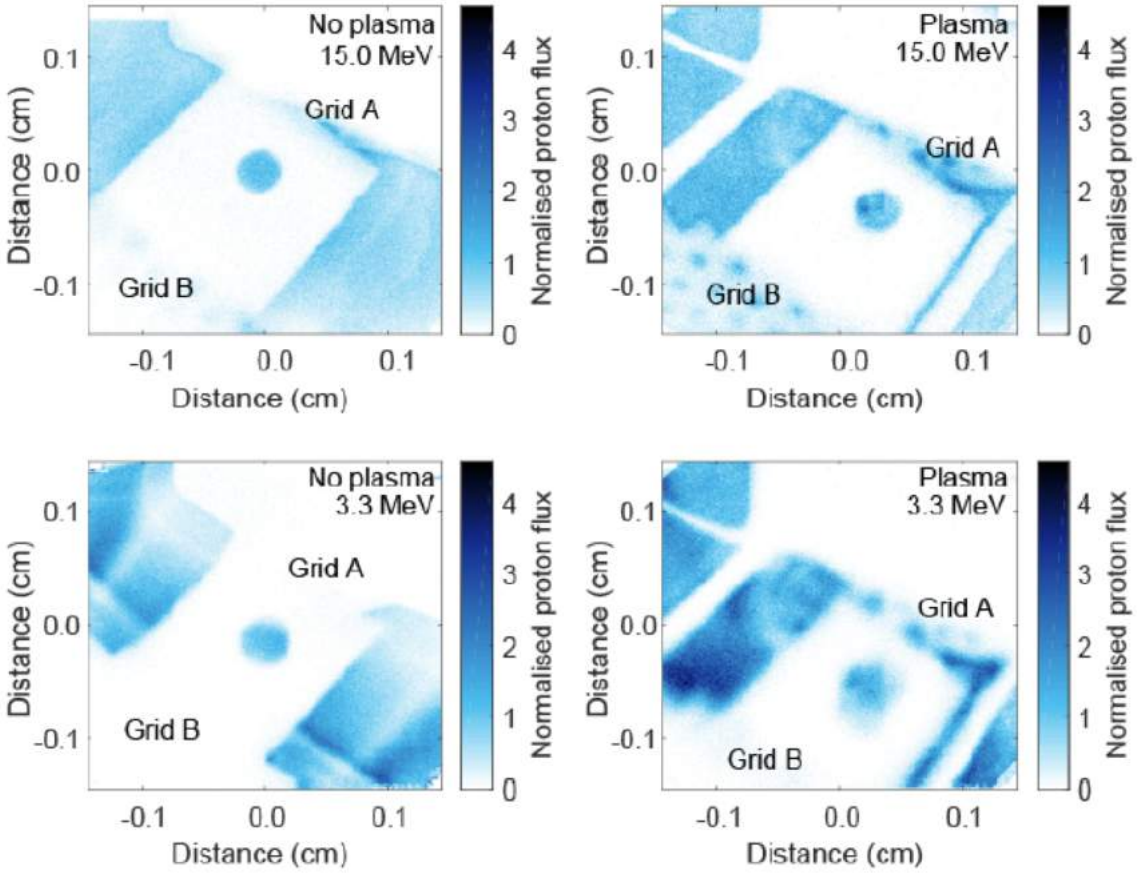

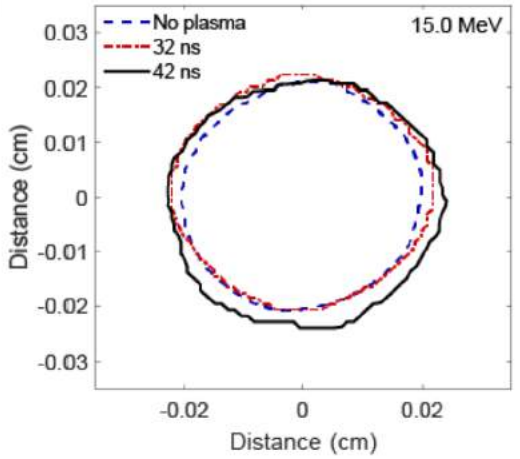

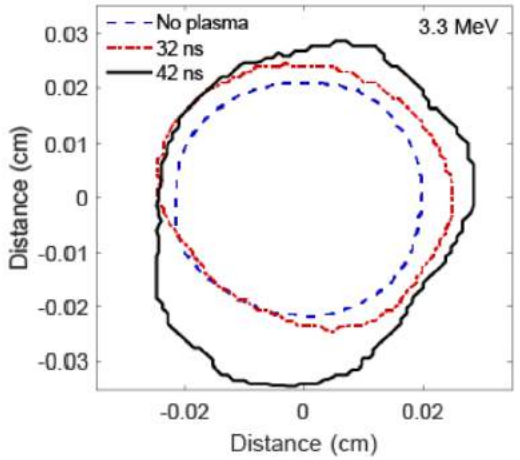

Magnetic fields in the Universe

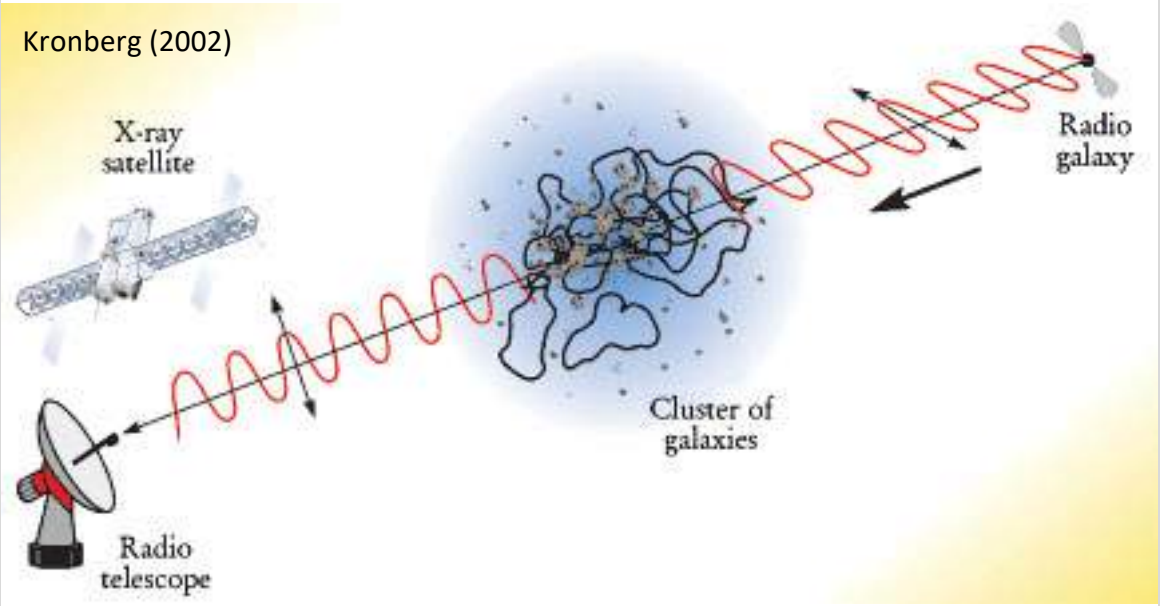

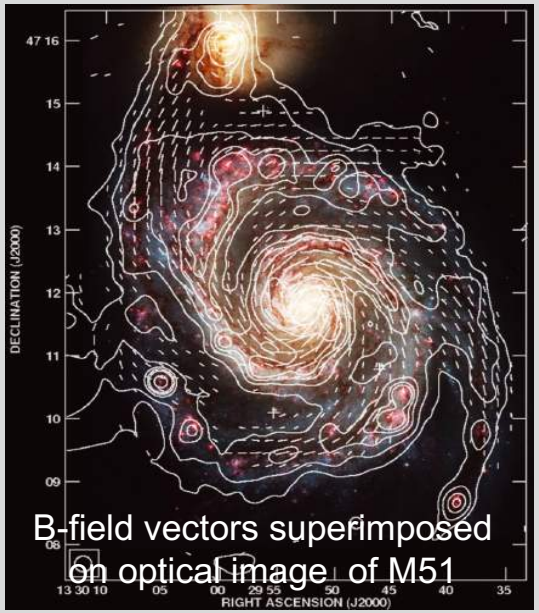

➜Faraday rotation and synchrotron emission are used to measure magnetic fields in galaxies and clusters.

➜The Universe is magnetised:

- Clusters and galaxies (a few μG)
- filaments (a few nG)
- voids (≈0.1 fG)

Cosmic generation of magnetic fields invokes MHD turbulence

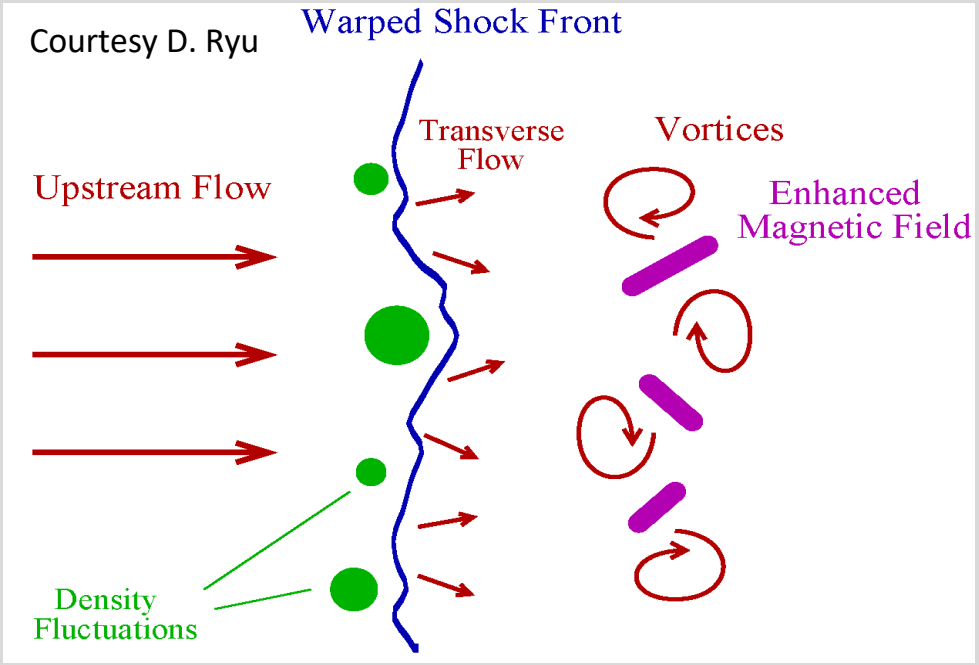

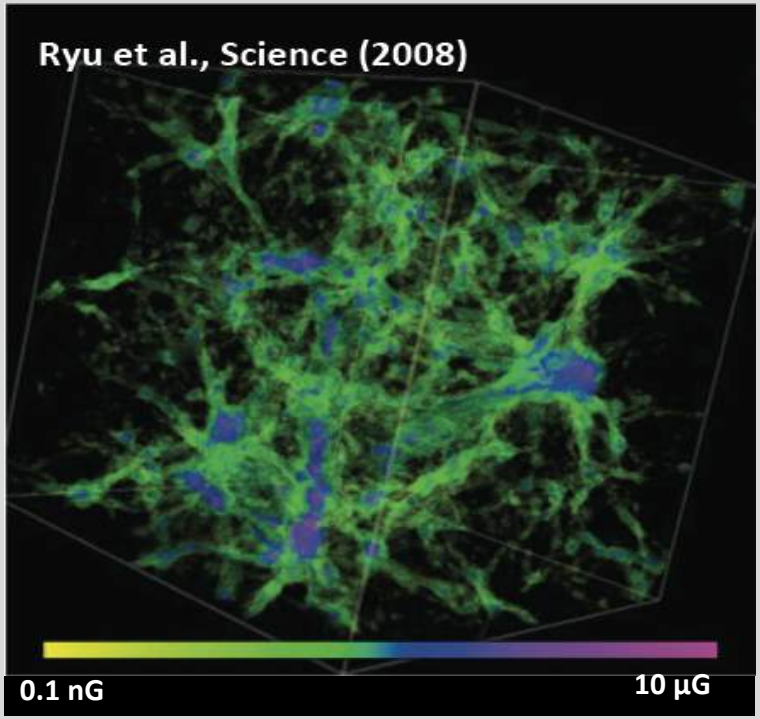

→Assume there are tiny magnetic fields generated before structure formation

→Magnetic field are then amplified to dynamical strength and coherence length by turbulent motions

Mechanisms for generating seed magnetic fields

➜ The induction equation requires a source term, otherwise $B(t=0)=0$ implies $B(t)=0$ for any times $t>0$

$$\frac{d\boldsymbol{B}}{dt} = \boldsymbol{u}\cdot\nabla\boldsymbol{B} + \frac{\eta c^2}{4\pi}\nabla^2\boldsymbol{B}$$

➜ Various mechanisms have been proposed (list *not* inclusive):

- Biermann's battery during structure formation (Kulsrud *et al*. 1997, Gregori et al. 2013)
- Weibel instability (Schlickheiser & Shukla 2003, Medvedev 2007)
- Resistive return current due to cosmic ray or photon drag (Miniati & Bell 2011, Langer *et al*. 2003)
- Interaction with a Nambu-Goldstone pseudo-scalar axion during the QCD cross-over (Miniati *et al*. 2018)

Biermann's battery mechanism occurs at curved shocks

Magnetic field is produced by misaligned T_e and n_e gradients

→ It develops on scales set by shocks in the interstellar medium

→ Structure formation simulations show that a tiny magnetic field is produced near shocks

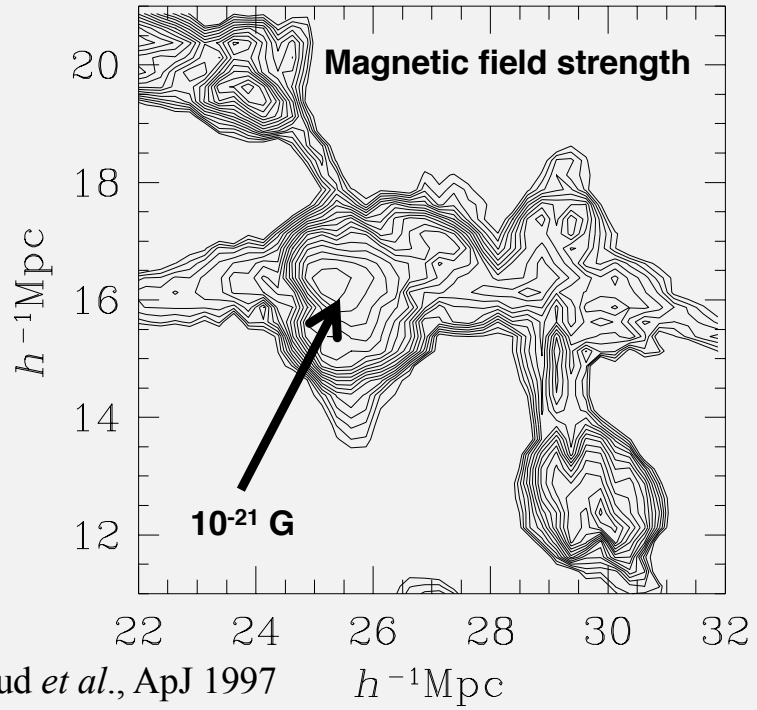

Kulsrud *et al.*, ApJ 1997

Laser plasma experiments can also generate magnetic fields at shocks

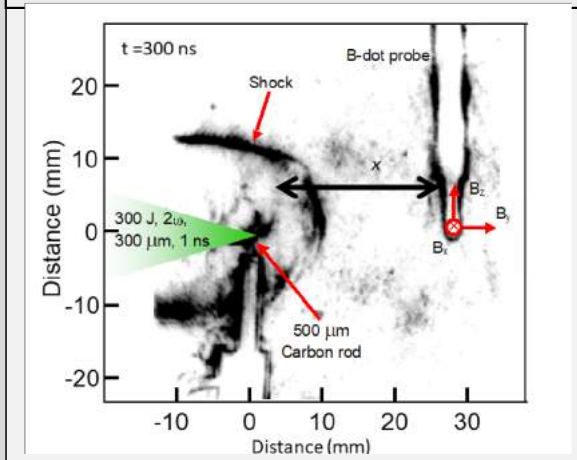

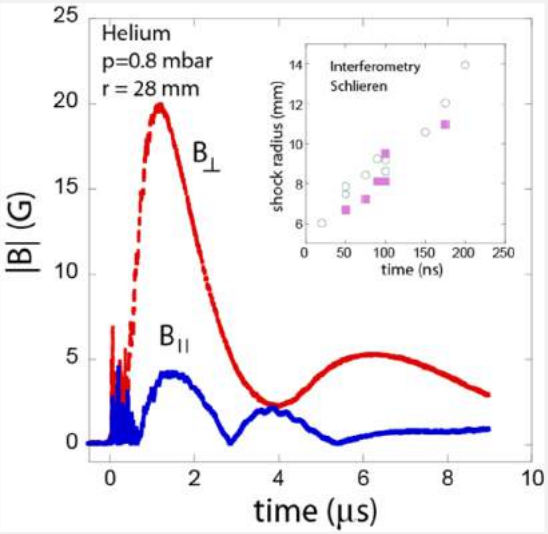

→ Expanding shock front follows a Sedov-Taylor blast wave relation

→ Magnetic field is measured as the shock arrives at the location of the induction probes

Gregori *et al.*, Nature 2012
Meinecke *et al.*, Nature Phys. 2014

Biermann's battery mechanism occurs at curved shocks

Magnetic field is produced by misaligned T_e and n_e gradients

→ It develops on scales set by shocks in the interstellar medium

→ Structure formation simulations show that a tiny magnetic field is produced near shocks

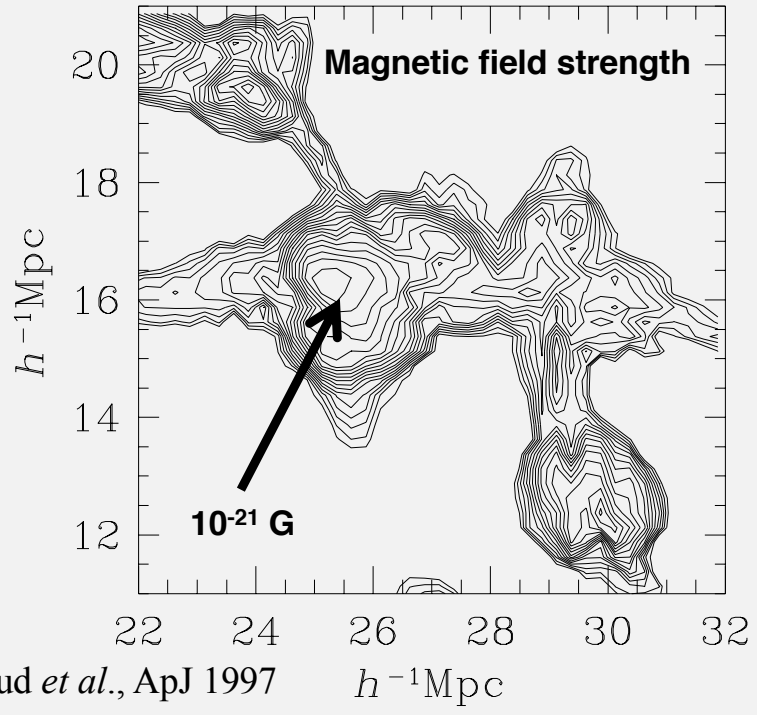

Kulsrud *et al.*, ApJ 1997

Laser plasma experiments can also generate magnetic fields at shocks

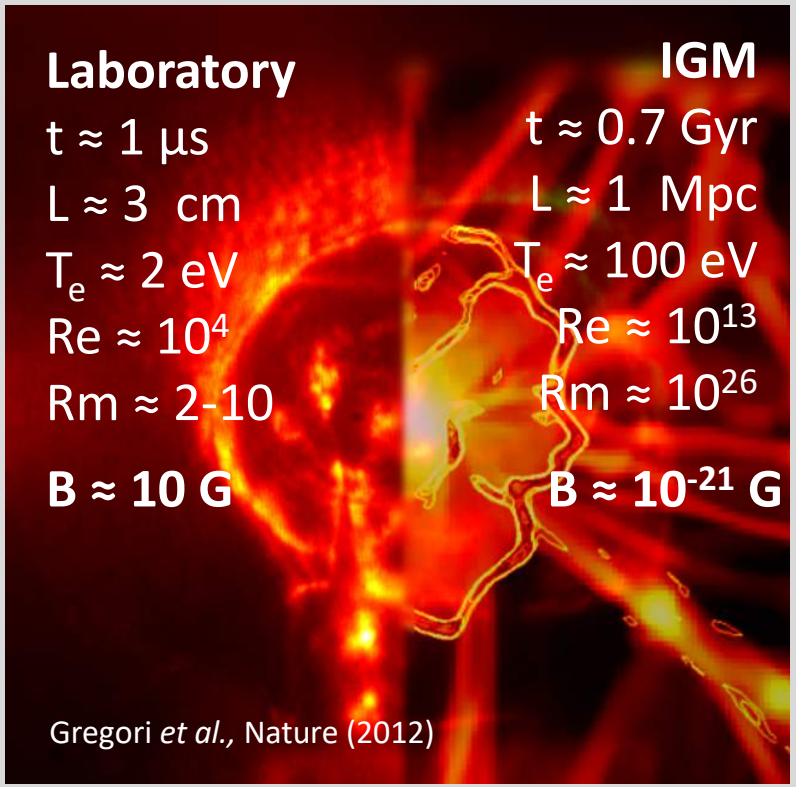

→ Magnetic fields scales with vorticity: $B \sim \omega \sim 1/t$

→ Scaled laboratory values are in agreement with structure formation simulations

Summary

Plasmas of astrophysical relevance can be investigated in the laboratory because of the *scale invariance* of the governing MHD equations

- E.g. cosmic magnetic fields can be produced by the 'Biermann Battery' and subsequently amplified by turbulent dynamo action
- Fusion protons can be produced inside the colliding streams and their momentum space diffusion can be measured
- Stochastic 2nd-order Fermi acceleration will *soon* be tested

We cannot yet make an universe in the laboratory …
but we can (nearly) make a supernova!

Thanks to all collaborators!

- Alex Rigby, Archie Bott, Laura Chen, **Konstantin Beyer**, Matthew Oliver, James Matthews, Jena Meinecke, Tony Bell, Alexander Schekochihin, **Gianluca Gregori**, Thomas White (Oxford)
- Petros Tzeferacos, Carlo Graziani, F Cattaneo, Don Lamb (Chicago)
- Dustin Froula, Joe Katz (LLE)
- Bruno Albertazzi, Michael Koenig (LULI)
- Fabio Cruz, Luis Silva (IST Lisbon)
- Steven Ross, Dmitri Ryutov, Hye-Sook Park (LLNL)
- Chi-Kang Li, Richard Petrasso (MIT)
- Dongsu Ryu (Unist)
- Sergey Lebedev (Imperial College)
- Francesco Miniati (ETH)
- Brian Reville (QUB)
- Cary Forest, Ellen Zweibel (Wisconsin)
- John Foster, Peter Graham (AWE)
- Alexis Casner (CEA)
- Nigel Woolsey (York)
- Ruth Bamford, Bob Bingham, Raoul Trines (Rutherford Appleton Laboratory)